The British Journal of Radiology, 79 (2006), 248–253

SHORT COMMUNICATION

Gold nanoparticles: a new X-ray contrast agent

[1]J F HAINFELD, PhD, [1]D N SLATKIN, MD, [1]T M FOCELLA, BS and [2]H M SMILOWITZ, PhD

[1]*Nanoprobes, Inc., 95 Horse Block Road, Yaphank, NY 11980 and* [2]*University of Connecticut Health Center, Farmington, CT 06030, USA*

ABSTRACT. There have been few fundamental improvements in clinical X-ray contrast agents in more than 25 years, and the chemical platform of tri-iodobenzene has not changed. Current agents impose serious limitations on medical imaging: short imaging times, the need for catheterization in many cases, occasional renal toxicity, and poor contrast in large patients. This report is the first demonstration that gold nanoparticles may overcome these limitations. Gold has higher absorption than iodine with less bone and tissue interference achieving better contrast with lower X-ray dose. Nanoparticles clear the blood more slowly than iodine agents, permitting longer imaging times. Gold nanoparticles, 1.9 nm in diameter, were injected intravenously into mice and images recorded over time with a standard mammography unit. Gold biodistribution was measured by atomic absorption. Retention in liver and spleen was low with elimination by the kidneys. Organs such as kidneys and tumours were seen with unusual clarity and high spatial resolution. Blood vessels less than 100 μm in diameter were delineated, thus enabling *in vivo* vascular casting. Regions of increased vascularization and angiogenesis could be distinguished. With 10 mg Au ml^{-1} initially in the blood, mouse behaviour was unremarkable and neither blood plasma analytes nor organ histology revealed any evidence of toxicity 11 days and 30 days after injection. Gold nanoparticles can be used as X-ray contrast agents with properties that overcome some significant limitations of iodine-based agents.

Received 4 February 2005
Revised 24 May 2005
Accepted 1 September 2005

DOI: 10.1259/bjr/13169882

Contrast agents for X-rays are based on tri-iodobenzene with substituents added for water solubility. Diatrizoate, an ionic form, was introduced in 1954, but the high osmolality of this compound (1.57 osm kg^{-1} for a 300 mg I ml^{-1} solution) was found to be the source of chemotoxicity [1]. In the 1970s, a non-ionic form, iohexol, lowered osmolality (0.67 osm kg^{-1}), and is still widely used today under the names Omnipaque® and Exypaque®, Amersham Health, Amersham, UK (now GE Healthcare). Because osmolality was still excessive, a dimeric form was introduced, iodixanol (Acupaque® and Visipaque®, Amersham Health, Amersham, UK (now GE Healthcare); 0.29 osm kg^{-1}). Intravascular agents based on other mid-Z to high-Z elements have not been successful due to toxicity, performance, or cost. The low molecular weights of the iodine agents (diatrizoate, 613; iohexol, 821; iodixanol, 1550) effect rapid renal clearance and vascular permeation, necessitating short imaging times. Intra-arterial catheterization is therefore commonly needed, but carries the risks of arterial puncture, dislodgement of plaque, stroke, myocardial infarction, anaphylactic shock and renal failure. A further shortcoming of the current agents is in molecular imaging, since their conjugates with antibodies or other targeting moieties fail to deliver iodine to desired sites at detectable concentrations.

Several other experimental X-ray contrast materials show promise as blood pool agents, including standard iodine agents encapsulated in liposomes [2, 3], a dysprosium-DTPA-dextran polymer [4], polymeric iodine-containing PEG-based micelles [5], perfluoroctyl bromide [6], dervatized polylysine linked to iodine [7], and iodine linked to a polycarboxylate core (P743, MW=12.9 kDa) [8]. Iron nanoparticles have been used successfully as MRI contrast agents [9], but our report is the first, to our knowledge, to use gold as an X-ray contrast agent *in vivo*.

With a higher atomic number (Au, 79 *vs* I, 53), and a higher absorption coefficient (at 100 keV: gold: 5.16 cm^2 g^{-1}; iodine: 1.94 cm^2 g^{-1}; soft tissue: 0.169 cm^2 g^{-1}; and bone: 0.186 cm^2 g^{-1}), gold provides about 2.7 times greater contrast per unit weight than iodine [10]. Imaging gold at 80–100 keV reduces interference from bone absorption and takes advantage of lower soft tissue absorption which would reduce patient radiation dose. Gadolinium has been used instead of iodine to image the chest with half the X-ray dose [11]. The higher molecular weight of nanoparticles (here ~50 kDa) permits much longer blood retention, so that useful imaging may be obtained after intravenous injection, possibly obviating invasive catheterization for diagnostic triage. Molecular imaging may also be possible as each nanoparticle bound to a targeting agent would deliver a ''truckload'' of ~250 gold atoms to a cognate

This study was supported in part by a National Cancer Institute Small Business Innovative Research Phase 1 Grant 1R43CA83576-01. JFH is part owner of Nanoprobes, Inc. Other authors do not have any financial interest.

receptor thereby increasing the signal. Although gold is more costly than iodine, low detectable amounts and significant benefits should enable feasible gold-mediated clinical radiography.

Materials and methods

Animals and injections

Balb/C mice were injected subcutaneously in the thigh with 10^6 EMT-6 syngeneic mammary carcinoma cells [12] suspended in 0.05 ml of equal volumes of medium and Matrigel. 10 days after tumour initiation, gold nanoparticles were injected via a tail vein. Experimental protocols using animals were approved by the University of Connecticut Health Center animal care committee.

Gold nanoparticles

1.9 ± 0.1 nm gold nanoparticles were obtained from Nanoprobes, Inc. (preparation # 1101, Yaphank, New York, USA). The size of the nanoparticles was determined by electron microscopy. The concentration of injected gold was 270 mg Au cm^{-3}, and volume injected was 0.01 ml g^{-1} mouse weight. Nanoparticles were suspended in phosphate-buffered saline at pH 7.4.

Gold analysis

Tissues were excised, placed in tared vials, and analysed for gold by graphite furnace atomic absorption spectrometry using a Perkin Elmer 4100Z instrument (Wellesley, Massachusetts, USA).

Radiographs

A Lorad Medical Systems mammography unit (Hologic, Inc., Danbury, CT; model XDA101827) was used with 8 mAs exposures (0.4 s at 22 kVp). Kodak Min-R2000 mammography film, 18 cm × 24 cm (Eastman Kodak, Rochester, NY) was used.

Toxicity tests

60 outbred CD1 mice (male and female) were randomized into four groups of 15 animals per group receiving 700 mg Au kg^{-1}, 70 mg Au kg^{-1}, or 7 mg Au kg^{-1}, or sham-injected with phosphate buffered saline. Animals were weighed and observed regularly for clinical signs. Animals were euthanized by CO_2 narcosis 1 day, 11 days, and 30 days after intravenous gold injections and ~0.4 ml blood was removed from the right ventricle immediately after the cessation of breathing. Haematology analytes included haematocrit, haemoglobin, total white [WBC] and red [RBC] blood cell counts, neutrophil, lymphocyte, monocyte, and eosinophil counts, mean corpuscular volume, mean corpuscular haemoglobin, mean corpuscular haemoglobin concentration, WBC differential (percent neutrophils, bands, lymphocytes, monocytes, and eosinophils), and blood smear microscopy. Blood chemistry analytes included glucose, blood urea nitrogen (BUN), creatine, calcium, phosphate, total protein, albumin, globin, albumin:globulin ratio, alanine aminotransferase (ALT), aspartate aminotransferase (AST), AST/ALT ratio, alkaline phosphatase, total bilirubin, and direct bilirubin. Livers and kidneys were weighed and slices of the following 24 tissues were prepared for microscopic study by formalin fixation, paraffin embedding, and haematoxylin/eosin staining: kidneys, liver, testes, epididymis, lungs, heart, adrenals, bone, bone marrow, spinal cord, sciatic nerves, oesophagus, stomach, duodenum, ileum, jejunum, colon, cecum, lymph nodes, spleen, thymus, trachea, ovaries, and uterus. Histopathology was evaluated by a board-certified veterinarian (A G Richter, DVM, DACVP) and assessed independently by a physician certified in anatomic pathology (D N Slatkin, MD, DABP).

Results

Gold nanoparticles, 1.9 nm in diameter, were suspended in phosphate-buffered saline and injected via a tail vein into Balb/C mice bearing EMT-6 subcutaneous mammary tumours. The vascular system was imaged in planar projection using a clinical mammography unit. Blood vessels as fine as 100 μm in diameter could be distinguished (Figure 1). A 5 mm tumour growing in one thigh was clearly evident from its increased vascularity and resultant higher gold content (Figure 1). These nanoparticles thus enable direct imaging, detection, and measurement of angiogenic and hypervascularized regions. Images taken at various times after intravenous injection show that the small nanoparticles do not concentrate in the liver and spleen, but clear through the kidneys (Figure 2). A closer examination of the kidneys revealed a remarkably detailed anatomical and functional display (Figure 3).

Toxicity and clearance are critical issues for clinical imaging. Mice intravenously injected with the gold nanoparticles at 2.7 g Au kg^{-1} survived over 1 year without signs of illness. The LD_{50} for this material is approximately 3.2 g Au kg^{-1}. In a 30-day toxicity study using 60 mice, intravenous injection of the gold nanoparticles (initially, 10 mg Au ml^{-1} blood) showed normal haematology (Table 1) and blood chemistry (Table 2). Histological examination of 24 vital organs and tissues from each mouse, assayed 11 days or 30 days after injection of the nanoparticles, showed no evidence of toxicity in any animals.

Quantitative pharmacokinetics using graphite furnace atomic absorption spectroscopy (Figure 4) showed that blood gold concentration decreased in a biphasic manner, with a 50% drop between 2 min and 10 min followed by a slower decrement of another 50% between 15 min and 1.4 h. The highest tissue gold concentration 15 min after injection was in the kidney (10.60 ± 0.2 percent of the injected dose per gram of measured tissue [%id/g]), followed by tumour (4.2 ± 0.4%id/g), liver (3.6 ± 0.3%id/g) and muscle (1.2 ± 0.1%id/g). Whole body gold clearance was 77.5 ± 0.4% of the total injected gold after 5 h. Muscles and blood were almost gold-free 24 h after injection (0.28 ± 0.07%id/g and 0.10 ± 0.01%id/g, respectively), whereas tumour at 24 h retained 64% of

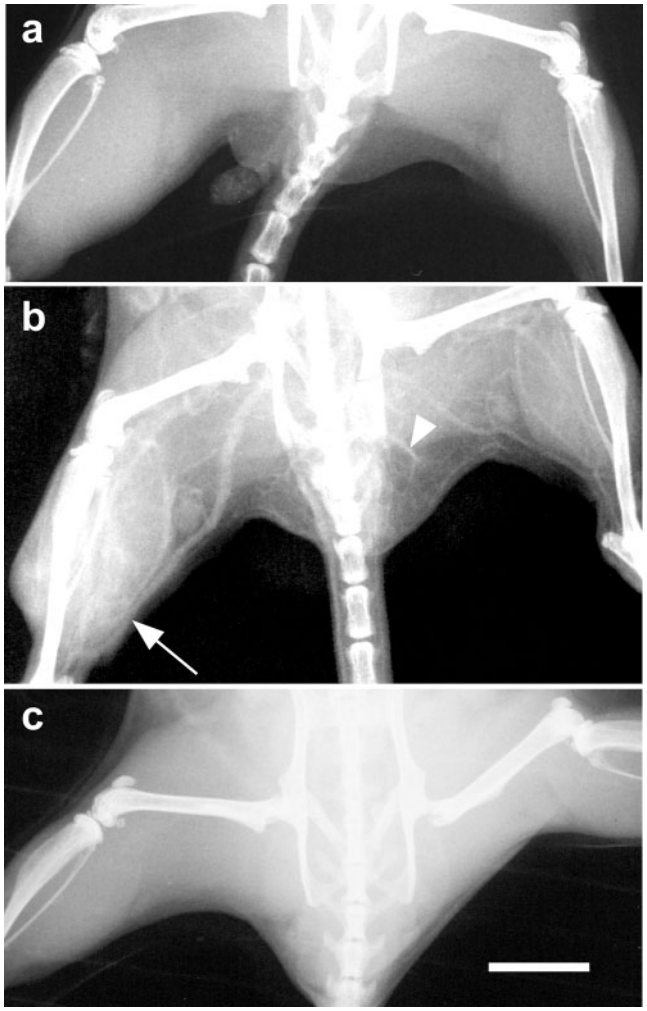

Figure 1. X-ray images mouse hind legs *in vivo*. (a) Before injection; (b) 2 min post tail vein injection of gold nanoparticles; (c) 2 min after equal weight of iodine contrast agent (Omnipaque®). Arrow points to leg with tumour and increased vascularity. Arrowhead points to 100 μm diameter vessel. Bar=5 mm. (Figures 1a and 1b are reproduced with permission from *Phys Med Biol* [12]).

its value reached at 15 min. The tumour:muscle gold ratio was 3.4 at 15 min post injection, improving to 9.6 at 24 h, enabling clear delineation of the tumour. In addition to imaging, higher tumour X-ray absorption due to the gold has been shown to greatly improve the efficacy of radiotherapy [13].

Even when concentrated, gold nanoparticle solutions were similar to water in viscosity, in sharp contrast to the high viscosity of iodine contrast media. The gold nanoparticles may be completely dried and later re-suspend easily in water or aqueous buffers, such as phosphate buffered saline, pH 7.4. Solubility was found to be at least 1.5 g Au ml^{-1}. The gold nanoparticles are stable, showing no change in spectra or aggregation after 6 months storage at 4℃ or −20℃.

Discussion

Gold's K-edge at 80.7 keV compared with iodine's at 33.2 keV confers higher absorptivity and ~3-fold better contrast at ~100 keV, a useful range for clinical CTs and fluoroscopes. Absorption is also higher at low energies (<30 keV), where mammography machines operate, again providing gold with an approximately 3-fold absorption advantage over iodine.

Some iodine agents' side effects are due to high osmolality. Iodine agents contain 3 (monomer) or 6 (dimer) iodine atoms per molecule. In contrast, the nanoparticles used here each contain about 250 gold atoms per molecule and at the same elemental concentration as iodine agents (350 mg Au ml^{-1}), therefore have a negligible osmolality of 0.0072 M. Saline could, of course, be added to provide iso-osmolality. The low viscosity of gold nanoparticle solutions would also facilitate injections.

Deliberately high amounts of gold were used to clarify printed images. CT is much more sensitive than planar imaging, and studies of high-Z agents indicate that good contrast-to-noise images can be obtained at gold concentrations of 100 μg ml^{-1} [14]. This level is ~100 times lower than a dose of gold nanoparticles at which we found no evidence of toxicity. Use of these lower amounts of gold clinically would not only improve the safety margin, but also lower the cost.

The extended imaging time and high contrast provided by gold nanoparticles after a non-toxic intravenous injection might enable such applications as: non-invasive imaging of coronary and cerebral arteries, assessment of atherosclerotic plaque and stenoses, delineation of stroke, arteriovenous malformations, aneurysms, renal angiography, determination of vascularity, and enhancement of mammography and virtual colonoscopy. Improved contrast might enable non-invasive detection of small tumours (*e.g.* < 1 cm) that are currently missed, yielding better prognoses. Tumour vascularity is correlated with invasiveness [15], so indices of vascularity make non-invasive staging possible. These gold nanoparticles might be useful to distinguish vulnerable plaque since it is more highly vascularized than stable plaque [16, 17]. With the advent of faster CT machines that lessen motion artefacts, gold-enhanced imaging of coronary arteries, especially those in obese patients or those with mural calcifications, might prove feasible via transvenous injection without resorting to arterial catheterization. Contrasting during transarterial catheterization might also benefit from the use of gold nanoparticles, especially for large patients where additional contrast is needed at present, since the concentration of gold can be made ~5 times higher than that of iodine agents. With the absorbance of gold 3 times higher at 100 keV, and the concentration 5 times higher (1.5 g Au cm^{-3} *vs* 0.3 g I cm^{-3}), the overall contrast gain could be greater than 10-fold.

The size of gold nanoparticles used here facilitates specific extravasation through angiogenic endothelium such as in tumours. This is evident from the extensive retention of gold in tumours after the blood has cleared, compared with the much lower accumulation in muscle (Figure 4). This gold retention may be useful for enhanced tumour detection and possibly for therapy due to the improved tumour:non-tumour ratio reached hours after injection.

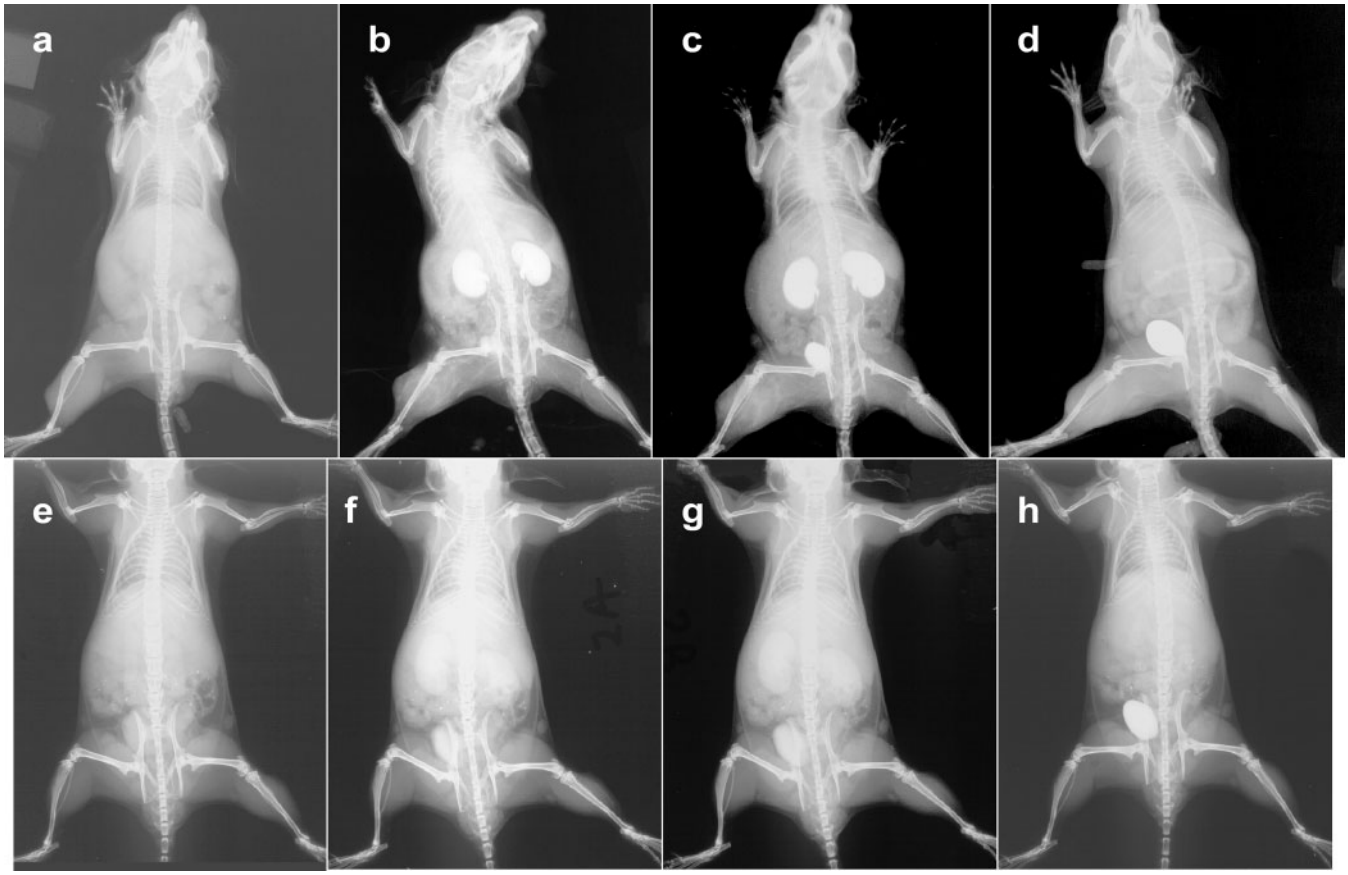

Figure 2. Pharmacokinetics of gold nanoparticles (a–d) and iodine contrast agent (e–h, Omnipaque®) in mice. (a,e) Before injection. (b,f) 2 min after injection; (c,g) 10 min after injection; (d,h) 60 min after injection. The gold nanoparticles show low liver and spleen uptake and clearance via kidneys and bladder (b–d). At 60 min (d), the contrast in the gold-injected mouse is similar to the uninjected mouse (a), indicating efficient clearance.

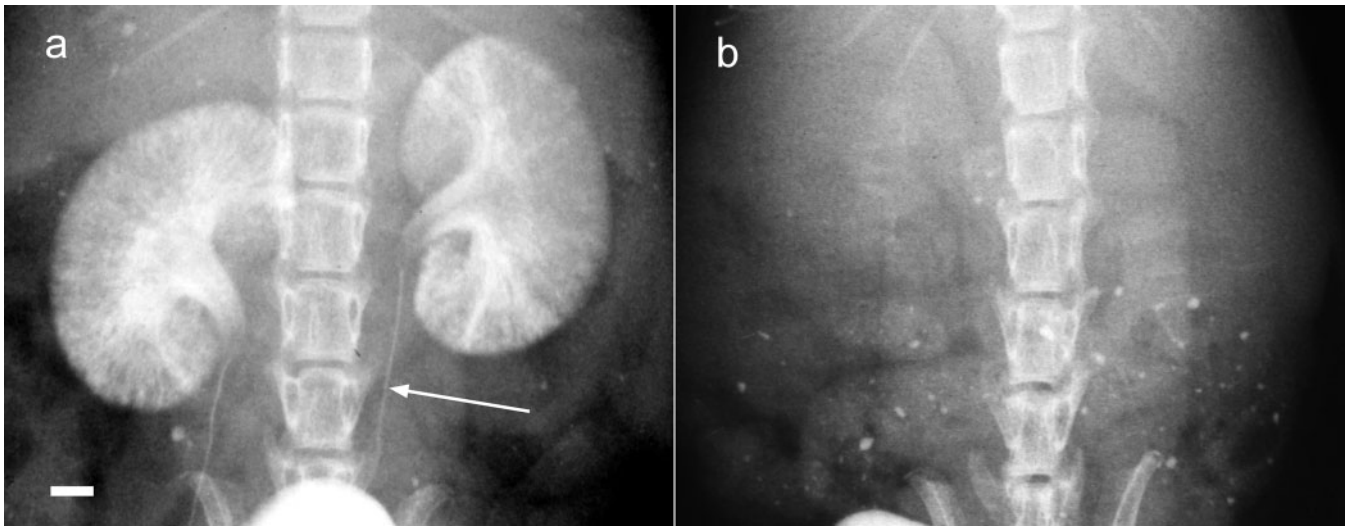

Figure 3. Planar X-ray image of kidneys in live mouse 60 min after intravenous injection of gold nanoparticles (a) or iodine contrast medium (b, Omnipaque®). Arrow points to 100 μm ureter. Bar=1 mm.

Conclusion

These animal studies demonstrate that gold nanoparticles are useful X-ray contrast agents that offer novel physical and pharmacokinetic advantages over current agents. They appear to be non-toxic and enable higher contrast and longer imaging times than currently possible using standard iodine-based agents.

Acknowledgments

We are indebted to Lahmer Lynds, PhD, Alexander Richter, MS, DVM, DACVP, Terry M Button, PhD, Bipin Jagjivan, MD, and Harold Atkins, MD for their expert advice and assistance. This study was supported in part by a National Cancer Institute Small Business Innovative Research Phase 1 Grant 1R43CA83576-01.

Table 1. Blood haematology of mice intravenously injected (0.2 ml) with an initial gold dose producing 10 mg Au ml^{-1} in the blood, sampled at day 1, 11, and 28, compared with mice sham injected with 0.2 ml phosphate buffered saline (control). Five animals were used per measurement, and all values were within normal limits

	Hct %	Hgb g dl^{-1}	WBC $\times$ 10^3	RBC $\times$ 10^6	RBC indices			% differential				
					MCV	MCH	MCHC	Bands	Neutro	Lymphs	Monos	Eosins
Day 1 Gold	44.3±4.9	15.7±1.2	5.4±3.5	9.0±0.7	49.3±1.9	17.5±0.5	35.6±1.3	0.2±0.4	45.0±13.0	54.0±13.0	0.4±0.5	0.4±0.5
Control	44.3±2.8	14.4±0.8	5.6±3.1	8.4±0.4	52.6±1.7	17.2±0.8	32.8±1.2	0.2±0.4	36.2±4.5	60.8±5.0	2.4±1.5	0.4±0.9
Day 11 Gold	42.2±2.9	14.9±0.9	9.2±2.6	9.2±0.6	45.6±1.9	16.1±0.6	35.3±0.6	0.0±0.0	11.2±7.0	87.6±7.3	0.4±0.5	0.8±1.3
Control	44.6±4.5	15.6±1.3	7.2±1.7	9.6±1.2	46.6±3.0	16.3±0.7	35.0±1.2	0.0±0.0	15.8±12.4	81.0±11.9	0.6±0.5	2.6±2.1
Day 28 Gold	39.8±1.5	14.8±0.4	8.0±4.0	8.7±0.5	45.4±0.6	16.9±0.6	37.1±0.8	0.0±0.0	36.8±8.5	60.6±10.7	60.6±10.7	2.4±3.0
Control	43.2±0.8	15.8±0.1	5.8±2.0	9.3±0.2	46.6±1.5	17.1±0.4	36.7±0.8	0.0±0.0	33.4±5.9	58.2±3.1	58.2±3.1	7.2±6.6

Hct, haematocrit; Hgb, haemoglobin; WBC, white blood cells; RBC, red blood cells; MCV, mean corpuscular volume; MCH, mean corpuscular haemoglobin; MCHC, mean corpuscular haemoglobin concentration; Neutro, neutrophils; Lymphs, lymphocytes; Monos, monocytes; Eosins, eosinophils.

Table 2. Serum clinical chemistry of mice intravenously injected (0.2 ml) with an initial gold dose producing 10 mg Au ml^{-1} in the blood, sampled at day 1, 11, and 28, compared with mice sham injected with 0.2 ml phosphate buffered saline (control). Five animals were used per measurement, and all values were within normal limits

	BUN mg dl^{-1}	CR mg dl^{-1}	GLU mg dl^{-1}	CA mg dl^{-1}	PO4 mg dl^{-1}	TP g dl^{-1}	ALB g dl^{-1}	GLB g dl^{-1}	A/G ratio	AST Units	ALT Units	AST/ALT ratio	ALP units	TBILI mg dl^{-1}
Day 1 Gold	30.8±6.7	0.2±0.1	341.6±83.7	11.7±0.7	13.9±3.7	6.0±0.8	4.3±0.6	1.8±0.3	2.5±0.5	368±698	362±274	4.2±4.2	174.4±39.3	0.2±0.1
Control	28.0±7.3	0.2±0.2	390.8±105.8	11.3±1.2	15.3±3.5	6.8±0.7	4.7±0.6	2.1±0.2	2.3±0.3	38.8±9.9	226±105	6.0±2.5	141.5±55.0	0.3±0.1
Day 11 Gold	28.4±6.7	0.4±0.5	319.6±47.7	11.6±0.6	12.3±2.0	6.3±0.3	4.5±0.5	1.8±0.3	2.6±0.7	58.8±8.9	96.0±10.6	1.7±0.2	157.6±25.7	0.2±0.0
Control	26.4±5.9	0.4±0.2	321.2±115.9	12.0±0.9	15.6±2.2	6.6±0.3	4.6±0.4	2.0±0.2	2.3±0.5	61.6±6.7	109.2±37.2	1.8±0.5	180.0±60.4	0.2±0.0
Day 28 Gold	28.4±4.3	0.0±0.1	389.5±77.8	10.7±1.4	13.0±1.4	6.0±0.3	4.0±0.1	1.9±0.3	2.1±0.3	60.4±17.1	33.6±7.3	2.0±1.2	139.6±32.5	0.2±0.0
Control	33.6±6.2	0.0±0.1	309.2±66.7	11.1±0.9	11.7±0.9	6.1±0.3	4.2±0.4	1.9±0.3	2.3±0.5	123.2±52.0	40.8±6.7	3.0±1.1	100.4±28.7	0.2±0.0

BUN, blood urea nitrogen; CR, creatine; GLU, glucose; CA, calcium; PO4, phosphate; TP, total protein; ALB, albumin; GLB, globin; A/G, albumin:globulin ratio; AST, aspartate aminotransferase; ALT, alanine aminotransferase; ALP, alkaline phosphatase; TBLI, total bilirubin.

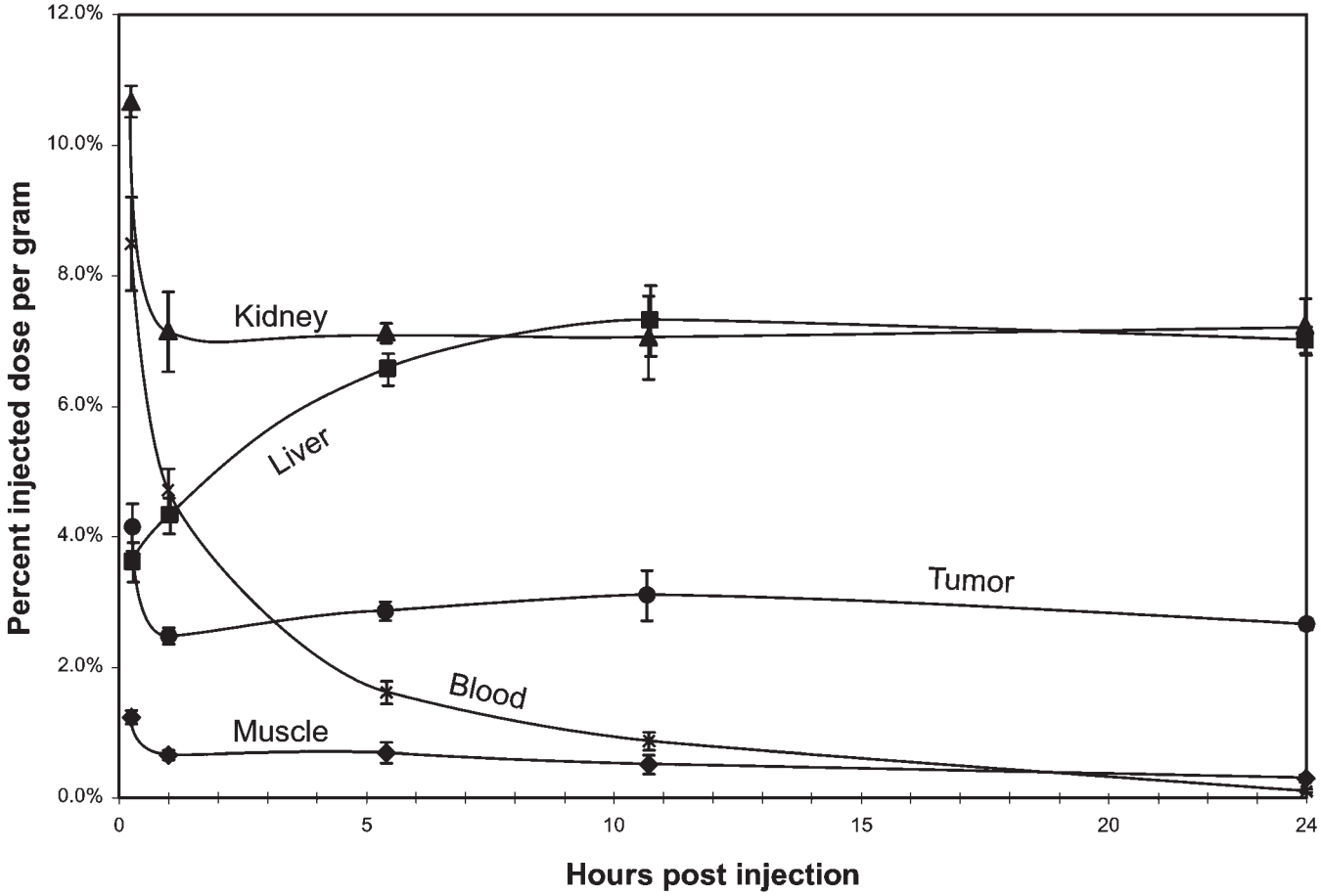

Figure 4. Pharmacokinetic data showing biodistribution of gold in mice following a 0.2 ml intravenous injection of gold nanoparticles showing percent injected dose per gram in the blood, kidneys, liver, muscle, and tumour over a 24 h period.

References

1. Yu S-B, Watson AD. Metal-based x-ray contrast media. Chem Rev 1999;99:2353–77.
2. Kao CY, Hoffman EA, Beck KC, Bellamkonda RV, Annapragada AV. Long-residence-time nano-scale liposomal iohexol for X-ray-based blood pool imaging. Acad Radiol 2003;10:475–83.
3. Schmiedl UP, Krause W, Leike J, Sachse A. CT blood pool enhancement in primates with -lopromide-carrying liposomes containing soy phosphatidyl glycerol. Acad Radiol 1999;6:164–9.
4. Vera DR, Mattrey RF. A molecular CT blood pool contrast agent. Acad Radiol 2002;9:784–92.
5. Torchilin VP. PEG-based micelles as carriers of contrast agents for different imaging modalities. Adv Drug Deliv Rev 2002;54:235–52.
6. Fruman SA, Harned RK 2nd, Marcus D, Kaufman S, Swenson RB, Bernardino ME. Perfluoroctyl bromide as a blood pool contrast agent for computed tomographic angiography. Acad Radiol 1994;1:151–3.
7. Torchilin VP, Frank-Kamenetsky MD, Wolf GL. CT visualization of blood pool in rats by using long-circulating, iodine-containing micelles. Acad Radiol 1999;6:61–5.
8. Idee JM, Port M, Robert P, Raynal I, Prigent P, Dencausse A, et al. Preclinical profile of the monodisperse iodinated macromolecular blood pool agent P743. Invest Radiol 2001;36:41–9.
9. Bulte JW, Kraitchman DL. Iron oxide MR contrast agents for molecular and cellular imaging. NMR Biomed 2004;17:484–99.
10. http://physics.nist.gov/PhysRefData/XrayMassCoef [Accessed 22 November 2005].
11. Atkins HL, Fairchild RG, Robertson JS, Greenberg D. Effect of absorption edge filters on diagnostic x-ray spectra. Radiology 1975;115:431–7.
12. Rockwell SC, Kallman RF, Fajardo LF. Characteristics of a serially transplanted mouse mammary tumor and its tissue-culture-adapted derivative. J Natl Cancer Inst 1972;49:735–49.
13. Hainfeld JF, Slatkin DN, Smilowitz HM. The use of gold nanoparticles to enhance radiotherapy in mice. Phys Med Biol 2004;49:N309–15.
14. Dilmanian FA, Wu XY, Parsons EC, Ren B, Kress J, Button TM, et al. Single-and dual-energy CT with monochromatic synchrotron x-rays. Phys Med Biol 1997;42:371–87.
15. Weidner N, Carroll PR, Flax J, Blumenfeld W, Folkman J. Tumor angiogenesis correlates with metastasis in invasive prostate carcinoma. Am J Pathol 1993;143:401–9.
16. Higuchi ML, Gutierrez PS, Bezerra HG, Palomino SA, Aiello VD, Silvestre JM, et al. Comparison between adventitial and intimal inflammation of ruptured and nonruptured atherosclerotic plaques in human coronary arteries. Arq Bras Cardiol 2002;79:20–4.
17. Tenaglia AN, Peters KG, Sketch MH Jr, Annex BH. Neovascularization in atherectomy specimens from patients with unstable angina: implications for pathogenesis of unstable angina. Am Heart J 1998;135:10–4.